# Effects of the ancillary ligands of polypyridyl ruthenium(II) complexes on the DNA-binding behaviors

**Hong Xu,[ab] Kang-Cheng Zheng,*[a] Hong Deng,[a] Li-Jun Lin,[a] Qian-Ling Zhang[b] and Liang-Nian Ji*[a]**

[a] *Department of Chemistry, Zhongshan University, Guangzhou 510275, P. R. China. E-mail: cesjln@zsu.edu.cn; Fax: 86-20-8403-5497; Tel: 86-20-8411-0115*

[b] *Department of Chemistry and Biology, Normal College, Shenzhen University, Shenzhen 518060, P. R. China. E-mail: xuhong@szu.edu.cn; Fax: 86-755-2653-4605; Tel: 86-755-2626-8581*

***Received (in Montpellier, France) 2nd January 2003, Accepted 9th April 2003***
***First published as an Advance Article on the web 2nd July 2003***



A new polypyridyl ligand PMIP {PMIP = 2-(4-methylphenyl)imidazo[4,5-*f*]1,10-phenanthroline}, and its Ru(II) complexes, $[Ru(bpy)_2PMIP]^{2+}$ **1** (bpy = 2,2′-bipyridine), $[Ru(phen)_2PMIP]^{2+}$ **2** (phen = 1,10-phenanthroline) and $[Ru(dmp)_2PMIP]^{2+}$ **3** (dmp = 2,9-dimethyl-1,10-phenanthroline), have been synthesized and characterized. The binding of the three complexes to calf thymus DNA (CT DNA) has been investigated with spectrophotometic methods, viscosity measurements, as well as equilibrium dialysis and circular dichroism spectroscopy. Complexes **1** and **2** can bind to CT DNA through intercalation. Complex **3** binds to CT DNA *via* partial intercalative mode. All the three complexes can enantioselectively interact with CT DNA in a way. Complex **3** is a much better candidate as an enantioselective binder to CT DNA than complex **1** and complex **2**. The *Δ* enantiomer of complex **1** is slightly predominant for binding to CT DNA to the *Λ* enantiomer. The experimental results suggest that the ancillary ligands of polypyridyl Ru(II) complexes have significant effects on the spectral properties and the DNA-binding behaviors of the complexes. On the basis of the experiments, the theoretical calculations applying the density functional theory (DFT) on the level of B3LYP/LanL2DZ basis set for these three complexes have been used to further discuss the trend in the binding strength or binding constants ($K_b$) of the complexes to DNA, as well as predict roughly some of their spectral properties.

## Introduction

The interaction between transition metal complexes and DNA has been extensively studied.[1] Binding studies of small molecules to DNA are very important in the development of new therapeutic reagents and DNA molecular probes.[2] Polypyridyl Ru(II) complexes can bind to DNA in a non-covalent interactions fashion such as electrostatic binding, groove binding,[3] intercalative binding and partial intercalative binding.[4] Many useful applications of these complexes require that the complexes bind to DNA through an intercalative mode. Therefore much work has been done on modifying the intercalative ligand,[5] and the influence of the ancillary ligands of the complexes has received little attention. Since the octahedral polypyridyl Ru(II) complexes bind to DNA in three dimensions, the ancillary ligands can also play an important role in governing DNA-binding of these complexes. So it is significant and interesting to find the effects of ancillary ligands on interaction and the binding mode of the complexes to DNA. To more clearly study the effects of ancillary ligands on DNA-binding behaviors of the polypyridyl Ru(II) complexes, the selection of intercalative ligand is also very important. An appropriate intercalative ligand is helpful to distinguishing the small differences of interaction of the complexes containing different ancillary ligands with DNA. In our laboratory, a series of similar Ru(II) complexes with PIP (PIP = 2-phenylimidazo[4,5-*f*]1,10-phenanthroline), a comparatively strong intercalative ligand,[4b] as the parent compound have been synthesized. In this paper, we select PMIP ligand {PMIP = 2-(4-methylphenyl)-imidazo[4,5-*f*]1,10-phenanthroline}, which is likely a moderate intercalative ligand because of the steric hindrance of the methyl group, as the intercalative ligand.

In addition, Ru(II) polypyridine complexes have also recently attracted the attention of many theoretical chemists.[6] More and more theoretical computations, especially for the computations applying the density functional theory (DFT) method[7] on Ru(II) and other transition metal complexes were reported,[8] because DFT can better consider electron correlation energies, obviously reduces the computation expenses and suits such kinds of singlet state complexes.[8d–8g] Recently, D. P. Rillema *et al.* suggested that the HOMO and LUMO distributions for Ru(II) two ring diimine complex cations from DFT calculations support the idea that the lowest energy transitions are metal-to-ligand charge transfer and that the LUMO energy for the mixed ligand complexes is mainly located on the ligand with the lowest LUMO energy in the corresponding complex $[RuL_3]^{2+}$.[8a] Y. Zhang *et al.* reported hydrolysis theory for cisplatin and its analogues based on density functional studies.[8b] N. Kurita and K. Kobayashi further reported density functional MO calculation for stacked DNA base-pairs with backbones.[6e] We also reported the studies on di-substitution effects, electron structures and related properties of some Ru(II) polypyridyl complexes with the DFT method.[8d–8g] These direct theoretical efforts on the level of molecular electronic structures of the complexes are also very significant in guiding experimental work.

We report herein the syntheses and characterization of a new polypyridyl ligand, PMIP and its Ru(II) complexes, $[Ru(bpy)_2PMIP]^{2+}$ **1** (bpy = 2,2′-bipyridine), $[Ru(phen)_2PMIP]^{2+}$ **2** (phen = 1,10-phenanthroline) and $[Ru(dmp)_2PMIP]^{2+}$ **3**

(dmp = 2,9-dimethyl-1,10-phenanthroline), the examination of their different DNA-binding behaviors, and the application of the DFT method to the explanation of the obtained experimental regularities or trends.

## Experimental

### Syntheses

1,10-phenanthroline-5,6-dione,[9] *cis*-$[Ru(bpy)_2Cl_2]\cdot 2H_2O$, *cis*-$[Ru(phen)_2Cl_2]\cdot 2H_2O$[10] and *cis*-$[Ru(dmp)_2Cl_2]\cdot 2H_2O$[11] were prepared according to literature procedures. Other reagents and solvents were purchased commercially and used without further purification unless otherwise noted.

**Caution.** Perchlorate salts of metal complexes with organic ligands are potentially explosive, and only small amounts of the material should be prepared and handled with great care.

**PMIP.** PMIP was synthesized by a method similar to the one described previously.[12] A mixture of 4-methylbenzaldehyde (3.5 mmol, 0.41 $cm^3$), 1,10-phenanthroline-5,6-dione (2.5 mmol, 0.525 g), ammonium acetate (50 mmol, 3.88 g) and glacial acetic acid (10 $cm^3$) was refluxed for about 2 h, then cooled to room temperature and diluted with water (*ca.* 25 $cm^3$). Dropwise addition of concentrated aqueous ammonia gave yellow precipitates, which were collected and washed with water. The crude products were purified by silica gel filtration (60–100 mesh, ethanol). The principal yellow band was collected. The solvent was removed by rotary evaporation, the products were collected, then were dried at 50 °C *in vacuo*. Yield 0.588 g, 76% (Found: C, 77.26; H, 4.63; N, 17.92%. Calc. for $C_{20}H_{14}N_4$: C, 77.42; H, 4.52; N, 18.06%). $^1$H NMR (DMSO-$d_6$): $\delta$13.56 (br, 1H), 9.03 (d, 2H), 8.95 (d, 2H), 8.21 (d, 2H), 7.82 (q, 2H), 7.41 (d, 2H), 2.42 (s, 3H). *m*/*z* 311 ($[M+1]^+$).

**$[Ru(bpy)_2PMIP](ClO_4)_2\cdot H_2O$ 1.** This complex was prepared by the following method. A mixture of *cis*-$[Ru(bpy)_2Cl_2]\cdot 2H_2O$ (0.5 mmol, 0.260 g), PMIP (0.5 mmol, 0.155 g), ethanol (10 $cm^3$) and water (5 $cm^3$) was refluxed under argon for 2 h to give a clear red solution. After most of the ethanol solvent was removed under reduced pressure, a red precipitate was obtained by dropwise addition of a saturated aqueous $NaClO_4$ solution. The product was purified by column chromatography on alumina using acetonitrile–toluene (1:1 v/v) as eluent and then dried *in vacuo*. Yield, 0.334 g, 71% (Found: C, 51.22; H, 3.69; N, 11.67%. Calc. for $C_{40}H_{32}Cl_2N_8O_9Ru$: C, 51.06; H, 3.40; N, 11.92%). $^1$H NMR (DMSO-$d_6$): $\delta$ 9.08 (d, 2H), 8.85 (q, 4H), 8.21 (t, 4H), 8.10 (t, 2H), 8.02 (d, 2H), 7.90 (q, 2H), 7.85 (d, 2H), 7.59 (m, 4H), 7.45 (d, 2H), 7.35 (t, 2H), 2.43 (s, 3H). *m*/*z* 723.4 ($[M-2ClO_4^-]^{2+}$), 823.1 ($[M-ClO_4^-]^+$).

**$[Ru(phen)_2PMIP](ClO_4)_2\cdot H_2O$ 2.** This complex (red) was synthesized in a manner identical to the one described for complex **1**, with 0.5 mmol, 0.284 g *cis*-$[Ru(phen)_2Cl_2]\cdot 2H_2O$ in place of *cis*-$[Ru(bpy)_2Cl_2]\cdot 2H_2O$. Yield, 0.316 g, 64% (Found: C, 53.68; H, 3.19; N, 11.13%. Calc. for $C_{44}H_{32}Cl_2N_8O_9Ru$: C, 53.44; H, 3.24; N, 11.34%). $^1$H NMR (DMSO-$d_6$): $\delta$ 9.06 (d, 2H), 8.77 (d, 4H), 8.39 (d, 4H), 8.21 (d, 2H), 8.12 (d, 2H), 8.07 (d, 2H), 8.00 (d, 2H), 7.79 (m, 2H), 7.76 (m, 4H), 7.47 (d, 2H), 2.43 (s, 3H). *m*/*z* 772 ($[M-2ClO_4^-+1]^{2+}$), 871 ($[M-ClO_4^-]^+$).

**$[Ru(dmp)_2PMIP](ClO_4)_2$ 3.** This complex (red) was synthesized in an identical manner to that described for complex **1**, with 0.5 mmol, 0.321 g *cis*-$[Ru(dmp)_2Cl_2]\cdot 2H_2O$ in place of *cis*-$[Ru(bpy)_2Cl_2]\cdot 2H_2O$. Yield, 0.344 g, 67% (Found: C, 56.03; H, 3.80; N, 10.87%. Calc. for $C_{48}H_{38}Cl_2N_8O_8Ru$: C, 56.14; H, 3.70; N, 10.92%). $^1$H NMR (DMSO-$d_6$): $\delta$ 8.90 (d, 2H), 8.80 (d, 2H), 8.43 (t, 4H), 8.24 (d, 2H), 8.15 (d, 2H), 7.97 (d, 2H), 7.38 (m, 4H), 7.32 (d, 2H), 7.22 (br, 2H), 2.29 (s, 3H), 1.83 (s, 6H), 1.70 (s, 6H). *m*/*z* 827 ($[M-2ClO_4^-]^{2+}$).

### Measurements

Elemental analyses (C, H and N) were carried out with a Perkin-Elmer 240C elemental analyzer. $^1$H NMR spectra were recorded on a Bruker DRX-500 NMR spectrometer with $(CD_3)_2SO$ as solvent and $SiMe_4$ as an internal standard. An LCQ electrospray mass spectrometer (ESMS, Finnigan) was employed for the investigation of charged metal complex species in methanol solvent. UV-Vis spectra were recorded on a Shimadzu UV-2501PC spectrophotometer. Emission spectra were determined with a Shimadzu RF-5301PC fluorescence spectrometer. The circular dichroism spectrum of the dialyzate was measured on a JASCO J-715 spectropolarimeter.

All the experiments involving interaction of the complex with DNA were conducted in twice distilled buffer containing tris(hydroxymethyl)-aminomethane (Tris, 5 mM) and NaCl (50 mM) and adjusted to pH 7.2 with hydrochloric acid. A solution of calf thymus DNA in the buffer gave a ratio of UV absorbance at 260 and 280 nm of about 1.8–1.9:1, indicating that the DNA was sufficiently free of protein.[13] The DNA concentration per nucleotide was determined by absorption spectroscopy using the molar absorption coefficient (6600 $M^{-1}\cdot cm^{-1}$) at 260 nm.[14]

Viscosity measurements were carried out using an Ubbdlodhe viscometer maintained at a constant temperature of 28.0 (±0.1) °C in a thermostatic bath. DNA samples with an approximate average length of 200 base pairs were prepared by sonication in order to minimize complexities arising from DNA flexibility.[15] Flow time was measured with a digital stopwatch. Each sample was measured three times and an average flow time was calculated. Data were presented as $(\eta/\eta_0)^{1/3}$ *versus* binding ratio ([Ru]/[DNA]),[16] where $\eta$ is the viscosity of DNA in the presence of complex and $\eta_0$ is the viscosity of DNA alone. Viscosity values were calculated from the observed flow time of DNA-containing solutions ($t > 100$ s) corrected for the flow time of buffer alone ($t_0$), $\eta = t - t_0$.

For the absorption spectra, equal solution of DNA was added to both complex solution and reference solution to eliminate the absorbance of DNA itself. The intrinsic binding constant $K_b$ of the complex to CT DNA was determined from the eqn. (1)[17] through a plot of $\frac{[DNA]}{\varepsilon_a-\varepsilon_f}$ *versus* [DNA].

$$\frac{[DNA]}{\varepsilon_a-\varepsilon_f}=\frac{[DNA]}{\varepsilon_b-\varepsilon_f}+\frac{1}{K_b(\varepsilon_b-\varepsilon_f)} \quad (1)$$

where [DNA] is the concentration of DNA in base pairs, $\varepsilon_a$, $\varepsilon_f$ and $\varepsilon_b$ are respectively the apparent extinction coefficient $\left(\frac{A_{obsd}}{[M]}\right)$, the extinction coefficient for free metal (M) complex and the extinction coefficient for the metal (M) complex in the fully bound form. In plots of $\frac{[DNA]}{\varepsilon_a-\varepsilon_f}$ *versus* [DNA], $K_b$ is given by the ratio of slope to intercept.

According to the classical Stern–Volmer equation:[18]

$$I_0/I = 1 + Kr \quad (2)$$

For the steady-state emission quenching experiment using $[Fe(CN)_6]^{4-}$ as quencher, where $I_0$ and $I$ are the fluorescence intensities in the absence and presence of $[Fe(CN)_6]^{4-}$, respectively. $K$ is a linear Stern–Volmer quenching constant dependent on the ratio of the bound concentration of the Ru(II) complex to the concentration of DNA. $r$ is the concentration of the quencher $[Fe(CN)_6]^{4-}$. For the steady-state competitive

binding experiment, $I_0$ and $I$ are the fluorescence intensities in the absence and presence of complex, respectively. Stern–Volmer quenching constant $K$ is dependent on the ratio of the bound concentration of EB to the concentration of DNA. $r$ is the ratio of total concentration of the complex to that of DNA ([Ru]/[DNA]). For both the emission quenching experiment and the competitive binding experiment, the Stern–Volmer quenching constant $K$ is given by the ratio of the slope to intercept in the plot of $I_0/I$ *versus* $r$.

The dialysis membrane was purchased from Union Carbide Co. and treated by means of the general procedure before use.[19] Equilibrium dialysis was carried out in the dark and held at 4 °C for 48 hours with 5 $cm^3$ of calf thymus DNA (1.0 mM) sealed in a dialysis bag and 10 $cm^3$ of the complexes (100 μM) outside the bag.

### Theoretical

Each of these three complexes forms from a Ru(II) ion, one main ligand or intercalated ligand (PMIP) and two ligands called ancillary ones (bpy, phen or dmp). The structural models and the corresponding $^1$H NMR spectra of the studied complexes are shown in Fig. 1. The full geometry optimization computations were performed for them, applying the DFT-B3LYP method[7] and LanL2DZ basis set,[20] and taking singlet state of the complexes.[21] All computations were performed with G98 quantum chemistry program-package.[22] In order to vividly depict the details of the frontier molecular orbital interactions, the stereographs of some related frontier molecular orbitals of the complexes were drawn with Molden v3.6 program[23] based on the obtained computational results.

## Results and discussion

### Viscosity studies

Hydrodynamic measurements that are sensitive to length change (*i.e.* viscosity and sedimentation) are regarded as the least ambiguous and most critical tests of a binding model in solution in the absence of crystallographic structural data.[24,25] A classical intercalation model demands that the DNA helix lengthens as base pairs are separated to accommodate the bound ligand, leading to the increase of DNA viscosity. In contrast, a partial, non-classical intercalation of ligand could bend (or kink) the DNA helix, reduce its effective length and, concomitantly, its viscosity.[24,25]

The effects of complexes **1**, **2** and **3** on the viscosity of DNA are shown in Fig. 2. For complexes **1** and **2**, the viscosity of DNA increases steadily with increasing concentration of the complex, and the extent of increase observed for complex **1** is smaller than that for complex **2**. By contrast, on increasing the amount of complex **3**, the relative viscosity of DNA decreases. The experimental results suggest that complexes **1** and **2** bind to DNA through a classical intercalation mode, complex **3** binds to DNA not by the classical intercalation mode but by the partial, non-classical intercalation model,

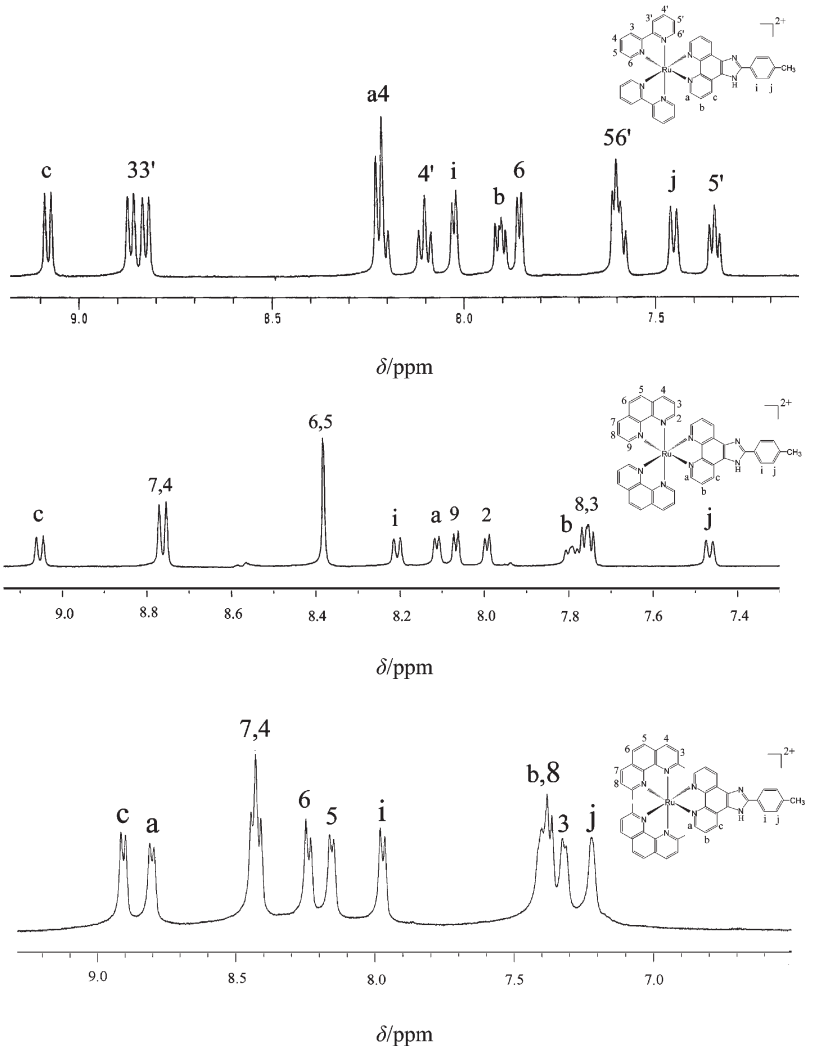


**Fig. 1** $^1$H NMR spectra of the aromatic region of complex **1** (top), complex **2** (middle) and complex **3** (bottom).

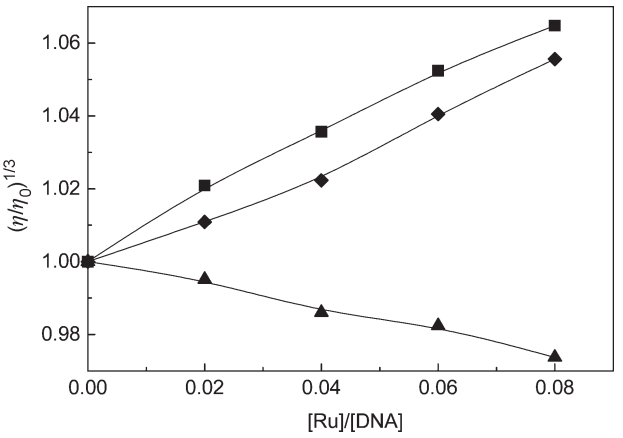


**Fig. 2** Effect of increasing amounts of complex **1** (◆), complex **2** (■) and complex **3** (▲) on the relative viscosities of CT DNA at 28.0 ± 0.1 °C. [DNA] = 0.5 mM.

and that complex **2** intercalated more strongly than complex **1**. This difference of DNA-binding mode between complexes **1**, **2** and complex **3** should be caused by their different ancillary ligands. Complex **1** or **2** containing the ancillary ligand bpy or phen can intercalate deeply into adjacent DNA base pairs. This would cause an extension in the helix and increase the viscosity of DNA. For complex **3**, due to the steric hindrance of the methyl groups located at the 2- and 9-positions of the phen ring in dmp ancillary ligand, the complex could not completely intercalate into DNA base pairs. The partial intercalation may act as a "wedge" to pry apart one side of a base-pair stack, as observed for the *Δ*-$[Ru(phen)_3]^{2+}$,[24,25] but not fully separate the stack as required by the classical intercalation mode. This would cause a static bend or kink in the helix and decrease the viscosity of DNA.

### Absorption spectroscopic studies

The electronic absorption spectra of complexes **1**, **2** and **3** mainly consist of two resolved bands. The low energy absorption band centered at 455–472 nm is assigned to metal-to-ligand charge transfer (MLCT) transition and the other band centered at 263–286 nm is attributed to intraligand (IL) π–π* transition by comparison with the spectrum of other polypyridyl Ru(II) complexes.[21] Fixed amounts (10 μM) of complexes **1**, **2** and **3** were titrated with increasing amounts of DNA. The electronic spectral traces are given in Fig. 3. For complex **1**, the absorption spectra show clearly that the addition of DNA to the complexes yields hypochromism about 28.9%, 20.6% and a red shift of 2, 4 nm at the ratio of [DNA]/[Ru] of 8 in the IL and MLCT band, respectively. As the DNA concentration is increased, for complex **2**, the hypochromism in the IL band reaches as high as 30.3% at 263 nm with 2 nm red shift at the ratio of [DNA]/[Ru] of 3. The MLCT band at 455 nm shows hypochromism about 14.2% and a red shift of 11 nm under the same experimental conditions. For complex **3**, upon addition of DNA, the IL band at 271.5 nm displays about 25.4% hypochromism with 1.5 nm red shift at the ratio of [DNA]/[Ru] of 10. The MLCT band at 466.5 nm exhibits hypochromism about 8.8% and a red shift of 6 nm under the same experimental conditions. Obviously, these spectral characteristics suggest that all the three complexes interact with DNA most likely through a mode that involves a stacking interaction between the aromatic chromophore and the base pairs of DNA.

To compare quantitatively the affinity of the three complexes bound to DNA, the intrinsic binding constants $K_b$ of these complexes to CT DNA were determined by monitoring the changes of absorbance in the IL band with increasing concentration of DNA using eqn. (1).[17] The intrinsic binding constant $K_b$ of complexes **1**, **2** and **3** were obtained about

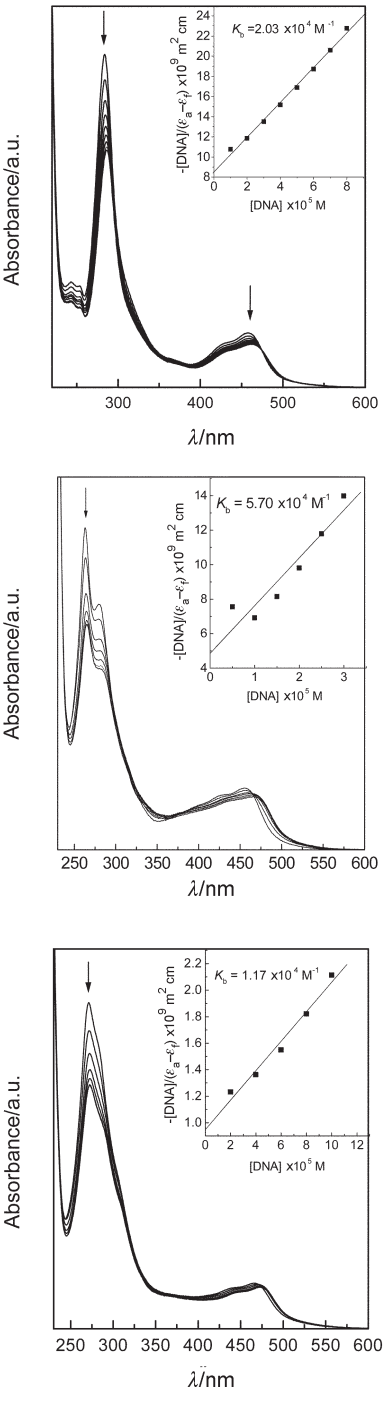


**Fig. 3** Absorption spectral of complex **1** (top), complex **2** (middle) and complex **3** (bottom) in Tris-HCl buffer upon addition of CT DNA with subtraction of the DNA absorbance. Arrow shows the absorbance changes upon increasing DNA concentrations. Inset: plots of [DNA]/($\varepsilon_a$–$\varepsilon_f$) *vs.* [DNA] for the titration of DNA with complexes; ■, experimental data points; full lines, linear fitting of the data.

$2.03 \times 10^4$ $M^{-1}$, $5.70 \times 10^4$ $M^{-1}$ and $1.17 \times 10^4$ $M^{-1}$, respectively. The results indicate that, as the ancillary ligand varies from phen, bpy to dmp, the DNA binding affinity of polypyridyl Ru(II) complexes declines. Similar case was observed in previous literature.[26] Comparing the intrinsic binding constant of the three complexes with that of those so-called DNA-intercalative Ru(II) complexes ($1.1 \times 10^4 - 4.8 \times 10^4$ $M^{-1}$),[27] these results of absorption spectroscopic studies support that of above viscosity studies, that is, complexes **1** and **2** bind to DNA by intercalation and complex **3** is close to the border between a classical intercalation and non-classical intercalation. These results may be explained by the fact that, for the

ancillary ligand, on going from bpy to phen, the plane area and hydrophobicity increase, leading to a greater binding affinity to DNA. On the other hand, for dmp ligand, substitution on the 2- and 9-positions of phen may cause severe steric constraints near the core of Ru(II) when the complex intercalates into the DNA base pairs. The methyl groups may come into close proximity of the base pairs at the intercalation site. These steric clashes then prevent the complex from intercalating effectively, and thus cause a diminution of the intrinsic binding constant.

### Fluorescence spectroscopic studies

Complexes **1** and **2** can emit luminescence in Tris buffer. Fixed amounts (10 μM) of complexes **1** and **2** were respectively titrated with increasing amounts of DNA, over a range of DNA concentrations from 10 to 200 μM. An excitation wavelength of 460 nm was used, and the total emission intensity was monitored at 590 nm. The results of the emission titrations for complex **1** and **2** with DNA are illustrated with the titration curves in Fig. 4. Upon addition of DNA, for complexes **1** and **2**, the emission intensity grows to around 1.53 and 1.78 times larger than that in the absence of DNA and saturates at a [DNA]/[Ru] ratio of 20, respectively. This implies that both the complexes can strongly interact with DNA and be protected by DNA efficiently, since the hydrophobic environment inside the DNA helix reduces the accessibility of solvent water molecules to the complex and the complex mobility is restricted at the binding site, leading to decrease of the vibrational modes of relaxation.

We can also derive the binding constants of the two complexes interacting with DNA from the emission spectra using the luminescence titration method.[24] The binding data obtained from the emission spectra were fitted using the McGhee and Von Hippel equation[28] to acquire the binding parameters. The intrinsic binding constants $K_b$ of $2.2(\pm0.1) \times 10^5$ $M^{-1}$ for complex **1** and $4.7(\pm0.3) \times 10^5$ $M^{-1}$ for complex **2** were determined, which are comparable to that observed for the similar complex $[Ru(bpy)_2MCP]^{2+}$ ($1.8 \times 10^5$ $M^{-1}$)[12] by the same method. Comparing with that obtained from absorption spectra, although the binding constants obtained from fluorescence with the McGhee–von Hippel method are different from those obtained from absorption with the method suggested by Wolfe *et al.*,[17] both sets of binding constants show that complex **2** binds to DNA more avidly than does complex **1**, and this difference between the two sets of binding constants should be caused by the different spectroscopy and the different calculation method. The binding size, $n$, was $1.85(\pm0.05)$ base pairs for complex **1** and $2.56(\pm0.05)$ base pairs for complex **2**, which are also similar to those of many Ru(II) polypyridine complexes.[29]

Steady-state emission quenching experiments using $[Fe(CN)_6]^{4-}$ as quencher are also used to observe the binding of the complexes to DNA. As illustrated in Fig. 5, in the absence of DNA, complex **1** and complex **2** were efficiently quenched by $[Fe(CN)_6]^{4-}$, resulting in a linear Stern–Volmer plot (slopes 4.18 and 5.39, respectively). In the presence of DNA, however, the slope of the plot is remarkably decreased and nearly equal to zero (slopes 0.11 and 0.03, respectively). This may be explained by the fact that the bound cations of complexes **1** and **2** are protected from the anionic water-bound quencher by the array of negative charges along the DNA phosphate backbone. The curvature reflects different degrees of protection or relative accessibility of bound cations. A larger slope for the Stern–Volmer curve parallels poorer protection and low binding. Therefore complex **2** binds to DNA more strongly than does complex **1**. Such a trend is consistent with the previous viscosity studies and absorption spectral results.

For complex **3**, no emission is observed either in the Tris buffer or in the presence of CT DNA. It also shows no photoluminescence examined in any of the organic solvents.

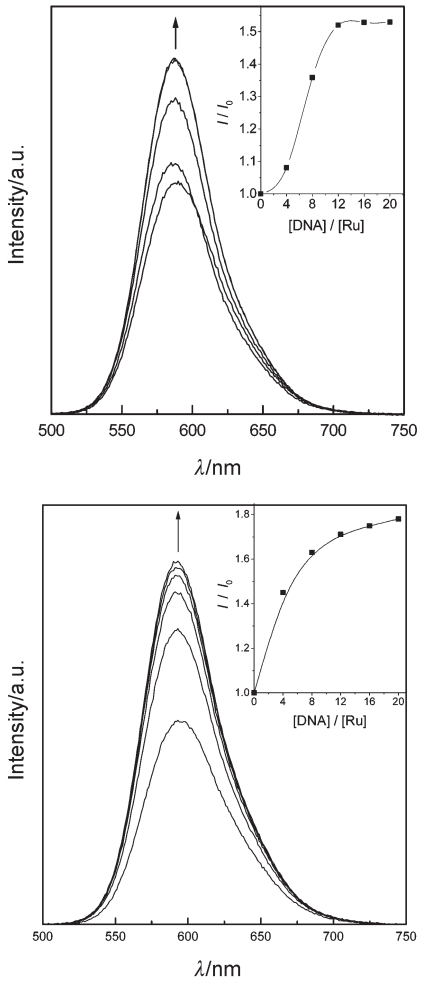


**Fig. 4** Emission spectra of complex **1** (top) and complex **2** (bottom) in Tris-HCl buffer in the absence and presence of CT DNA. Arrow shows the intensity changes upon increasing DNA concentrations. Inset: plots of relative integrated emission intensity *versus* [DNA]/[Ru].

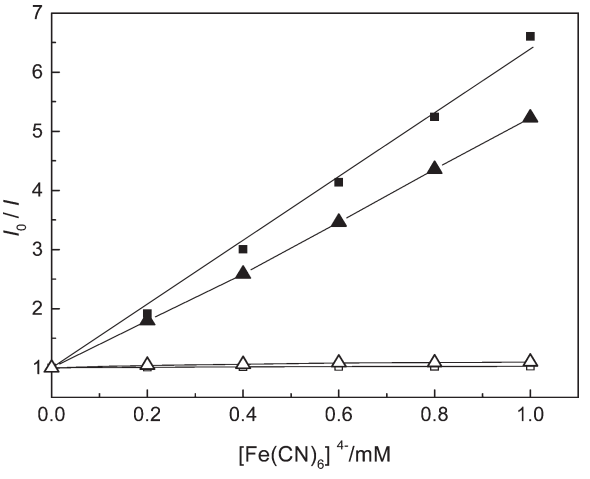


**Fig. 5** Emission quenching curves of complex **1** and complex **2** with increasing concentration of quencher $[Fe(CN)_6]^{4-}$ in the absence (for complex **1** shown as ▲ and complex **2** shown as ■) and presence (for complex **1** shown as △ and complex **2** shown as □) of CT DNA. [Ru] = 4 μM, [DNA]/[Ru] = 40.

This could be caused by a reduced ligand field making the excited states accessible. The reduced ligand field is firmed by the computed coordination bond lengths (Ru–N), which are 0.2124 nm (main-ligand) and 0.2157 nm (co-ligand) for complex **3**, and 0.2105 nm and 0.2106 nm for complex **2** and 0.2108 nm and 0.2097 nm for complex **1** respectively. Some computed frontier molecular orbital energies were also listed in Fig. 6. They show that the energy of LUMO for complex **3** is much higher than that for complexes **1** and **2**, so the excited state of complex **3** should be unstable, and can easily return to the ground state through nonradiative energy dissipation. Similar cases were observed for this type of Ru(II) complex.[26,30] Steady-state competitive binding experiments using complex **3** as quencher may give further information about the binding of the complex to DNA. As we know, ethidium bromide (EB) emits intense fluorescence light in the presence of DNA. It was previously reported that the enhanced fluorescence can be quenched, at least partially by the addition of a second molecule.[18,31] The extent of quenching fluorescence of EB bound to DNA is used to determine the extent of binding between the second molecule and DNA. The emission spectra of EB bound to DNA in the absence and the presence of complex **3** are shown in Fig. 7. The fluorescence quenching curve of DNA-bound EB by complex **3** (inset in Fig. 7) illustrates that the quenching of EB bound to DNA by complex **3** is in good agreement with the linear Stern–Volmer equation. This also proves that the partial replacement of EB bound to DNA by $[Ru(dmp)_2PMIP]^{2+}$ results in a decrease of the fluorescence intensity.

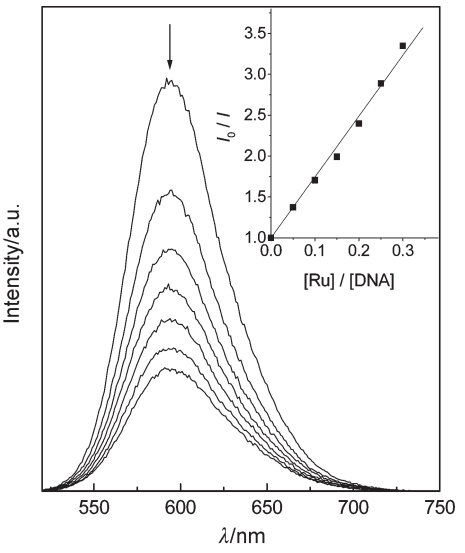


**Fig. 7** Emission spectra of EB bound to DNA in the presence of complex **2**. [EB] = 20 μM, [DNA] = 100 μM, [Ru]/[DNA] = 0, 0.05, 0.10, 0.15, 0.20, 0.25 and 0.30. Arrow shows the intensity changes upon increasing concentrations of the complexes. Inset: Fluorescence quenching curve of DNA-bound EB by complex **2**.

### Enantioselective binding

Equilibrium dialysis experiments may offer the opportunity to examine the enantioselectivity of complexes binding to DNA. Racemic solutions of the three complexes were dialyzed against CT DNA for 48 hours and then subjected to CD analysis. The CD spectra in the UV region of the dialysates of complexes **1**, **2** and **3** are shown in the top of Fig. 8. All the dialysates of complexes **1**, **2** and **3** show CD signals. The CD signals for complexes **1** and **2** are weak, which shows that the extents of preferential enantiomeric binding for complexes **1** and **2** are small.

Complex **1** has been resolved into its pure enantiomers. The CD spectra of the enantiomers of complex **1** in the UV region are shown in the bottom of Fig. 8. For complex **1**, the exhibited CD spectra were assigned to the *Λ* form, as judged by comparison with the CD spectra of its enantiomers. This indicates that the *Δ* form is slightly predominant for binding to CT DNA to the *Λ* enantiomer. According to the proposed binding model,[30,32] the *Δ* enantiomer of the complex, a right-handed propeller-like structure, will display a greater affinity than

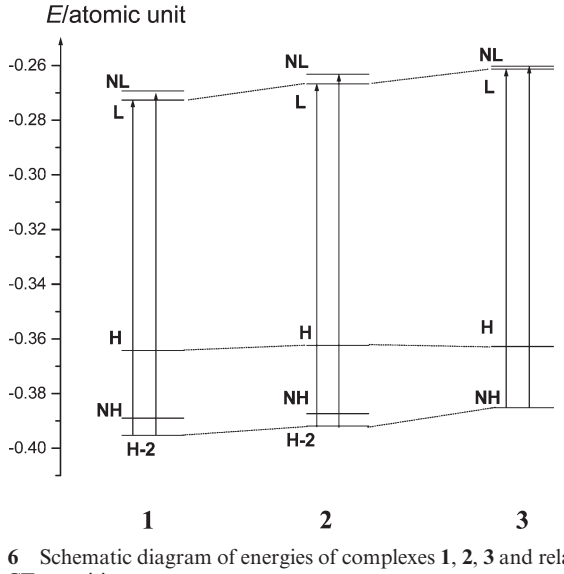


**Fig. 6** Schematic diagram of energies of complexes **1**, **2**, **3** and related $^1$MLCT transition.

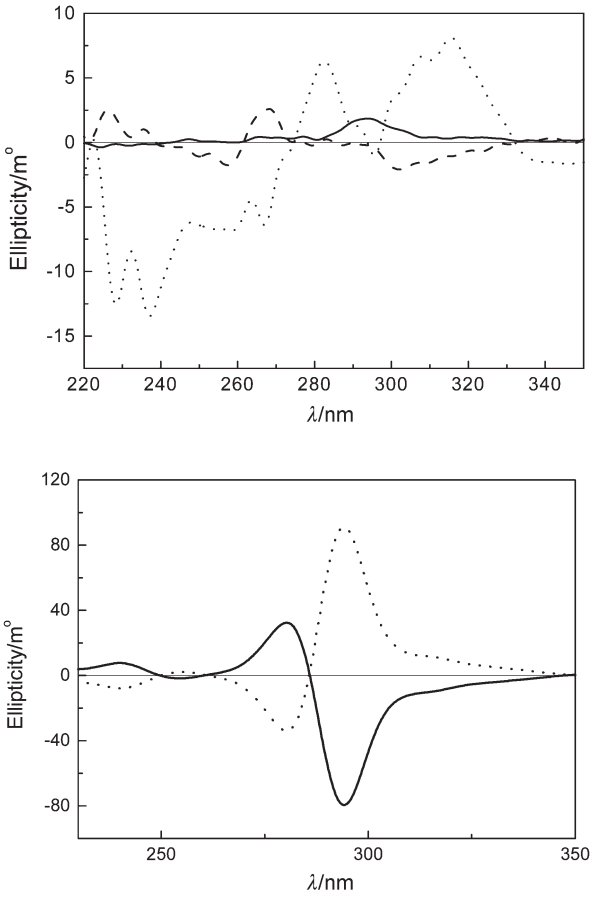


**Fig. 8** Circular dichroism spectra of the dialysates of complex **1** (full lines), complex **2** (broken lines) and complex **3** (dotted lines) after 48 h dialysis against calf thymus DNA ([Ru] = 100 μM, [DNA] = 1.0 mM) (top). Circular dichroism spectra of the *Δ* form (full lines) and the *Λ* form (dotted lines) of complex **1** (bottom).

the $\Lambda$ enantiomer with the right-handed calf thymus DNA helix, due to the appropriate steric matching. Our results may give evidence to support this proposal.

The CD signals of complex **3** are much stronger than those of complexes **1** and **2**, and the CD signals of complex **2** are in opposition to those of complex **3**. The stronger CD signals of complex **3** suggest the larger difference between interactions of its two isomers with DNA. It is likely that, for the weakly DNA-binding complex **3**, since the steric hindrances of the methyl groups substituted at dmp ligand have a very significant effect on one of the isomers binding to DNA, this leads to a special preference for the other isomer binding to DNA. On the basis of the previous reported document,[33] we speculate that, for the complexes that have analogous structures, the same type of isomers of those complexes should have analogous CD signals. The CD spectra of complex **2** and complex **3** suggest that, as compared with complex **2**, the different type of isomer of complex **3** strongly interacts with DNA enantioselectively. This should also be caused by the steric hindrances of the methyl groups in dmp ligand.

Although complexes **2** and **3** have not been resolved into their pure enantiomers, and we can not determine which enantiomer binds to DNA enantioselectivly, for each of the three complexes, it is certain that complex **3** is a much better candidate as an enantioselective binder to CT DNA than complexes **1** and **2**, and that the ancillary ligands have a significant influence on the interaction of the enantioselectivity of polypyridyl Ru(II) complexes with DNA.

### Theoretical explanation of trends in DNA-binding and spectral properties of complexes

As well-known, there are π–π interactions in the DNA-binding of these complexes in intercalation mode. But up to now, a whole DNA molecule, in particular, the supermolecular system formed from DNA and a metal complex is too large in size to be calculated, therefore, it is very important and necessary to theoretically estimate the interaction between both from their individual electronic structural characteristics.

The above-mentioned trends in DNA-binding and spectral properties can be explained by our theoretical computations with DFT method and the frontier molecular orbital theory.[34] Some computed frontier molecular orbital energies, the schematic diagram of the max ($\lambda$) $^1$MLCT transition, and the stereographs of the related frontier molecular orbitals of the three complexes were given in Table 1, Fig. 6 and Fig. 9 respectively. According to the frontier molecular orbital theory, a higher HOMO energy of one reactant molecule and a lower LUMO energy of the other are advantageous to the reaction between the two molecules, because electrons more easily transfer from the HOMO of one reactant to the LUMO of the other in the orbital interaction. A simple calculation model and computed results by the DFT method for stacked DNA base-pairs with backbones have been reported by Noriguki Kruita *etc.*[6e] It should be a better simplified approximation model for DNA, and thus should be useful and feasible for such a purpose. The energies of the HOMO and 6 occupied MOs lying near the HOMO for the CG/CG stacking calculated by the authors were −1.27, −1.33, −1.69, −1.79, −1.98, −2.06 and −2.08 eV, respectively, and the components of HOMO and NHOMO were mainly distributed on base-pairs. We have also performed some calculations for the Ru(II) complexes using the DFT method in this field, and the calculated energies of their LUMOs and 14 unoccupied MOs lying near the LUMOs are within in the range of −7.42 to −4.71 eV for $[Ru(bpy)_2PMIP]^{2+}$, −7.26 to −4.67 eV for $[Ru(phen)_2PMIP]^{2+}$ and −7.1 to −4.66 eV for $[Ru(dmp)_2PMIP]^{2+}$, and the components of these MOs distribute predominantly on ligands, in particular, on main-ligands or called intercalative ligands. It can be clearly seen that the energies of the HOMO and the occupied orbitals lying near the HOMO of the DNA model are all much higher than those of the LUMO and 14 unoccupied MOs lying near the LUMO of every one of the three complex cations. We believe such a trend in the relative energies to be kept even though the orbital energies for the CG/CG stacking were replaced by those for the other base-pair stacking, because the attraction of metal complex cations with high positive charges for electrons in the frontier MOs is much stronger than that of various DNA. Lower LUMO energy of the complex in the intercalation mode should be advantageous to accept the electron from base-pairs of DNA, so that the LUMO energies of the complexes should be an important factor (but not the only one) correlating to their DNA-binding constants. The experimental results show that the trend in DNA-binding constants ($K_b$) is $K_b(\mathbf{2}) > K_b(\mathbf{1}) > K_b(\mathbf{3})$. It can be explained as follows: $K_b(\mathbf{3})$ is the smallest because of $\varepsilon_L(\mathbf{3})$ is the greatest. As for $K_b(\mathbf{2}) > K_b(\mathbf{1})$, although $\varepsilon_L(\mathbf{2}) > \varepsilon_L(\mathbf{1})$ to certain extent, the hydrophobicity of the phen ligand is greater than that of the bpy ligand, and thus it makes the area of the main ligand intercalating into DNA increase for the corresponding complex. As a result, $K_b(\mathbf{2}) > K_b(\mathbf{1})$ when synthetically considering both the LUMO energy factor and the hydrophobicity effect of the ancillary ligand.

From Fig. 9, we can also clearly see that for the complexes **1** and **2**, the max ($\lambda$) singlet metal to ligand charge-transfer ($^1$MLCT) bands should correspond to the electron transitions from their HOMOs-2 to LUMOs respectively, whereas that for complex **3** should correspond to the electron transition from its NHOMO to LUMO according to the molecular orbital components of the complexes.

Since in absorption and emission spectra of the Ru(II) complexes, the corresponding energy change between presence and absence of DNA is smaller, and no special pattern changes in the absorption or emission spectra of Ru(II) complexes in the presence of DNA have been detected, except increases in luminescence intensity for emission spectra and hypochromism for absorption spectra, we consider that there is not a greater effect on the corresponding orbitals for the complexes binding to DNA (relative to free complexes). This further suggests that the interaction between the series of complexes and DNA should be a weak one between molecules, so that the properties of $^1$MLCT electron transition bands in these Ru(II) complexes binding to DNA should be unchanged, in accordance with experiment.

**Table 1** Some frontier molecular orbital energies ($\varepsilon_I$/atomic unit) of the complexes (1 atomic unit = 27.21 eV)

| Complex | Occ[a] | Occ | Occ | HOMO | LUMO | Vir[b] | Vir | $\Delta\varepsilon_{L-H}$ | $\Delta\varepsilon_{L-NH}$ | $\Delta\varepsilon_{L-(H-2)}$ |
|---|---|---|---|---|---|---|---|---|---|---|
| **1** | −0.4000 | −0.3953 | −0.3890 | −0.3643 | −0.2726 | −0.2693 | −0.2627 | 0.0917 | 0.1146 | 0.1227 |
| **2** | −0.3960 | −0.3919 | −0.3874 | −0.3624 | −0.2667 | −0.2632 | −0.2600 | 0.0957 | 0.1207 | 0.1252 |
| **3** | −0.3888 | −0.3880 | −0.3852 | −0.3628 | −0.2613 | −0.2602 | −0.2563 | 0.1015 | 0.1239 | — |

[a] Occ: Occupied molecular orbital; HOMO (or H): The highest Occ. [b] Vir: Virtual molecular orbital; LUMO (or L): The lowest Vir.

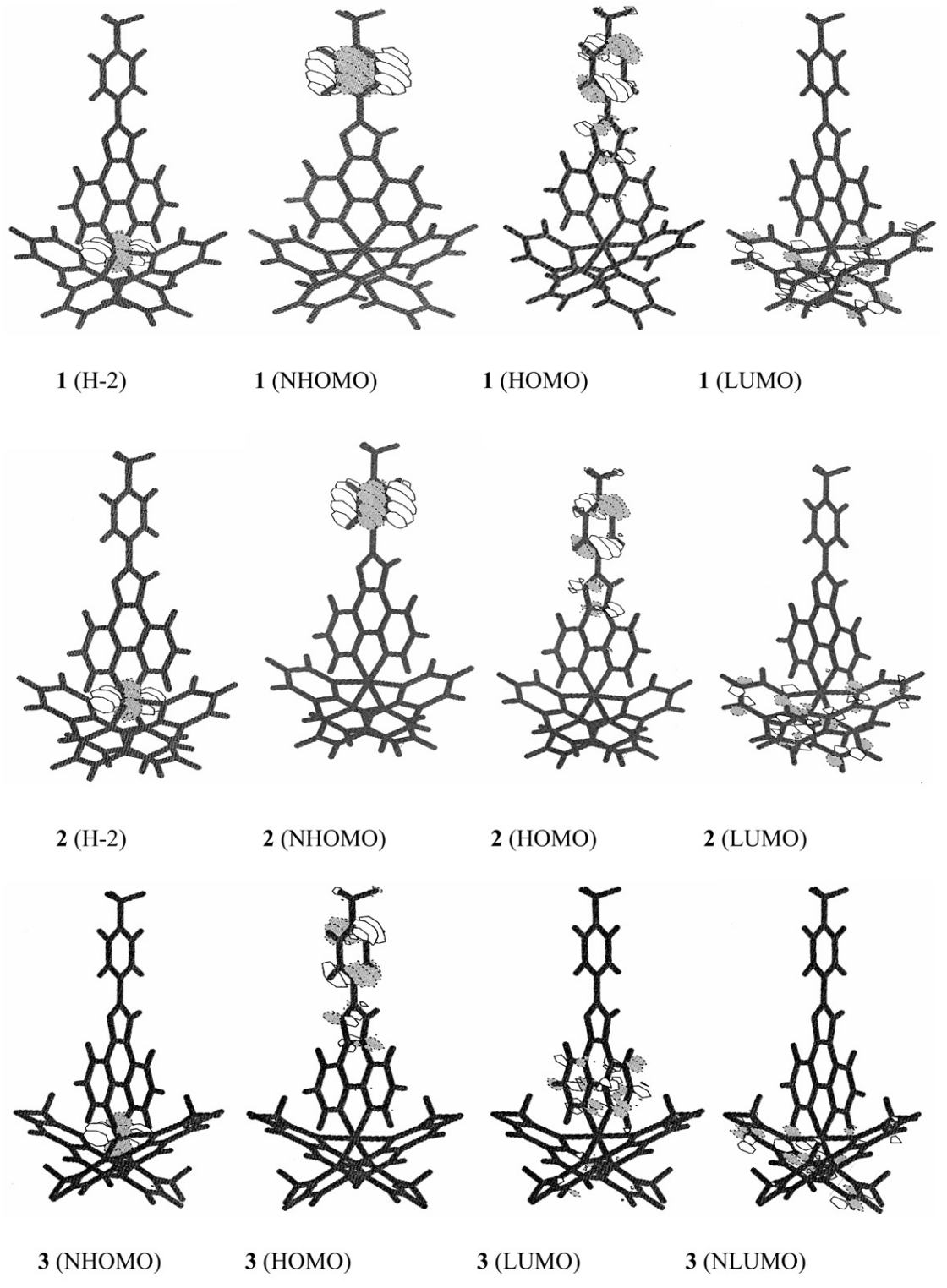


**Fig. 9** Some related frontier molecular orbital stereographs of complexes **1**, **2** and **3**.

## Conclusions

Spectroscopic studies, viscosity measurements together with equilibrium dialysis and circular dichroism spectroscopy show that complex **1** and complex **2** can bind to CT DNA through intercalation, complex **3** binds to CT DNA *via* a partial intercalative mode, all the three complexes can interact with CT DNA enantioselectively in a way, complex **3** is a much better candidate as an enantioselective binder to CT DNA than complexes **1** and **2**, and that the *Δ* enantiomer of complex **1** is slightly predominant over the *Λ* enantiomer for binding to CT DNA. The experimental results suggest that the ancillary ligands of polypyridyl Ru(II) complexes have significant effects on the spectral properties and the DNA-binding behavior of the complexes. The increase of ancillary ligand size increases its hydrophobicity, facilitating interaction with DNA. However, if the ancillary ligand is too large, its steric hindrance would interfere with the depth of intercalation into the base pair of DNA. The theoretical calculation results applying DFT method can also be used to further discuss the trend in the binding strength or binding constants ($K_b$) of the complexes to DNA as well as to roughly predict some of their spectral properties.

## Acknowledgements

We are grateful for the support of the National Natural Science Foundation of China, the Research Fund of Royal Society of Chemistry U.K., the Natural Science Foundation of Guangdong Province, the State Key Laboratory of Coordination Chemistry in Nanjing University and the State Key Laboratory of Bio-organic, Natural Products Chemistry in Shanghai Institute of Organic Chemistry.

## References

1 L. N. Ji, X. H. Zou and J. G. Liu, *Coord. Chem. Rev.*, 2001, **216–217**, 513.
2 B. A. Jackson, V. Y. Alekseyev and J. K. Barton, *Biochemistry*, 1999, **38**, 4655; P. J. Dandlier, R. E. Holmlin and J. K. Barton, *Science*, 1997, **274**, 1465; D. B. Hall, R. E. Holmlin and J. K. Barton, *Nature*, 1996, **382**, 731; C. J. Murphy and J. K. Barton, *Methods Enzymol.*, 1993, **226**, 576; D. S. Sigman, A. Mazumder and D. M. Perrin, *Chem. Rev.*, 1993, **93**, 2295; F. M. O'Reilly and J. M. Kelly, *New J. Chem.*, 1998, **22**, 215; E. Bernal-Méndez, J. S. Sun, F. González-Vílchez and M. Leng, *New J. Chem.*, 1998, **22**, 1479; L. Mishra, A. K. Yadaw, S. Srivastava and A. B. Patel, *New J. Chem.*, 2000, **24**, 505.
3 G. Yang, J. Z. Wu, L. Wang, L. N. Ji and X. Tian, *J. Inorg. Biochem.*, 1997, **66**, 141.
4 (*a*) J. G. Liu, B. H. Ye, H. Li, L. N. Ji, R. H. Li and J. Y. Zhou, *J. Inorg. Biochem.*, 1999, **73**, 117; (*b*) J. Z. Wu, B. H. Ye, L. Wang, L. N. Ji, J. Y. Zhou, R. H. Li and Z. Y. Zhou, *J. Chem. Soc., Dalton Trans.*, 1997, **21**, 1395; (*c*) Y. Xiong, X. F. He, X. H. Zou, J. Z. Wu, X. M. Chen, L. N. Ji, R. H. Li, J. Y. Zhou and K. B. Yu, *J. Chem. Soc., Dalton Trans.*, 1999, **23**, 19.
5 Y. Xiong and L. N. Ji, *Coord. Chem. Rev.*, 1999, **189**, 1.
6 (*a*) N. V. Ivanova, O. V. Sizov, A. B. Nikolskii and A. I. Panin, *J. Struct. Chem.*, 1999, **40**, 620; (*b*) O. V. Sizova, A. I. Panin, N. V. Ivanova and V. I. Batanovskii, *J. Struct. Chem.*, 1997, **38**, 366; (*c*) M. K. Nazeeruddin, S. M. Zakeeruddin, R. Humphry-Baker, S. I. Gorelsky, A. B. P. Lever and M. Gratzel, *Coord. Chem. Rev.*, 2000, **208**, 213; (*d*) M. Ziegler and A. V. Zelewsky, *Coord. Chem. Rev.*, 1998, **177**, 257; (*e*) N. Kurita and K. Kobayashi, *Comput. Chem.*, 2000, **24**, 351.
7 P. Hohenberg and W. Kohn, *Phys. Rev. B*, 1964, **136**, 864; A. D. Becke, *J. Chem. Phys.*, 1993, **98**, 1372; A. Gorling, *Phys. Rev.*, 1996, **A54**, 3912; J. B. Foresman and Æ. Frisch, *Exploring Chemistry with Electronic Structure Methods*, 2nd edn., Gaussian Inc., Pittsburgh PA, USA, 1996.
8 (*a*) S. R. Stoyaner, J. M. Villegas and D. P. Rillema, *Inorg. Chem.*, 2002, **41**, 2941; (*b*) Y. Zhang, Z. J. Guo and X. Z. You, *J. Am. Chem. Soc.*, 2001, **123**, 9378; (*c*) D. Reha, M. Kabelac, F. Ryjacek, J. Sponer, J. E. Sponer, M. Elstner, S. Suhai and P. Hobza, *J. Am. Chem. Soc.*, 2002, **124**, 3366; (*d*) K. C. Zheng, J. P. Wang, W. L. Peng, X. W. Liu and F. C. Yun, *J. Phys. Chem. A*, 2001, **105**, 10 899; (*e*) K. C. Zheng, J. P. Wang, X. W. Liu, Y. Shen and F. C. Yun, *J. Mol. Struct.: TheoChem.*, 2002, **577**, 95; (*f*) K. C. Zheng, J. P. Wang, Y. Shen, W. L. Peng and F. C. Yun, *Dalton Trans.*, 2002, 111; (*g*) K. C. Zheng, Y. Shen, J. P. Wang, X. W. Liu and F. C. Yun, *Inorg. Chim. Acta*, 2002, **335C**, 100; (*h*) A. Pfletschinger, W. Koch and H. G. Schmalz, *Chem. Eur. J.*, 2001, **7**, 5325; (*i*) V. B. Javoslav, S. Jiri and L. Jerzy, *Phys. Chem. Chem. Phys.*, 2001, **3**, 4404; (*j*) N. H. Damrauer, B. T. Weldon and J. K. McCusker, *J. Phys. Chem. A*, 1998, **102**, 3382; (*k*) S. Tobisch, T. Nowak and H. Bögel, *J. Organomet. Chem.*, 2001, **619**, 24.
9 E. Amouyal, A. Homsi, J. C. Chambron and J. P. Sauvage, *J. Chem. Soc., Dalton Trans.*, 1990, **14**, 1841.
10 B. P. Sullivan, D. J. Salmon and T. J. Meyer, *Inorg. Chem.*, 1978, **17**, 3334.
11 J. P. Collin and J. P. Sauvage, *Inorg. Chem.*, 1986, **25**, 135.
12 Y. Xiong, X. H. Zou, J. H. Wu, L. N. Ji, R. H. Li, J. Y. Zhou and K. B. Yu, *Transition Met. Chem.*, 1999, **24**, 263.
13 J. Marmur, *J. Mol. Biol.*, 1961, **3**, 208.
14 M. E. Reichmann, S. A. Rice, C. A. Thomas and P. Doty, *J. Am. Chem. Soc.*, 1954, **76**, 3047.
15 J. B. Chaires, N. Dattagupta and D. M. Crothers, *Biochemistry*, 1982, **21**, 3933.
16 G. Cohen and H. Eisenberg, *Biopolymers*, 1969, **8**, 45.
17 A. Wolfe, G. H. Shimer and T. Meehan, *Biochemistry*, 1987, **26**, 6392.
18 J. R. Lakowicz and G. Webber, *Biochemistry*, 1973, **12**, 4161.
19 J. K. Barton, J. J. Dannenberg and A. L. Raphael, *J. Am. Chem. Soc.*, 1984, **106**, 2172.
20 P. J. Hay and W. R. Wadt, *J. Chem. Phys.*, 1985, **82**, 270; P. J. Hay and W. R. Wadt, *J. Chem. Phys.*, 1985, **82**, 299.
21 A. Juris, V. Balzani, F. Barigelletti,Campagna, S. Campagna, P. Belser and A. V. Zelewsky, *Coord. Chem. Rev.*, 1988, **84**, 85.
22 M. J. Frisch, G. W. Trucks, H. B. Schlegel, G. E. Scuseria, M. A. Robb, J. R. Cheeseman, V. G. Zakrzewski, J. A. Montgomery, Jr., R. E. Stratmann, J. C. Burant, S. Dapprich, J. M. Millam, A. D. Daniels, K. N. Kudin, M. C. Strain, O. Farkas, J. Tomasi, V. Barone, M. Cossi, R. Cammi, B. Mennucci, C. Pomelli, C. Adamo, S. Clifford, J. Ochterski, G. A. Petersson, P. Y. Ayala, Q. Cui, K. Morokuma, N. Rega, P. Salvador, J. J. Dannenberg, D. K. Malick, A. D. Rabuck, K. Raghavachari, J. B. Foresman, J. Cioslowski, J. V. Ortiz, A. G. Baboul, B. B. Stefanov, G. Liu, A. Liashenko, P. Piskorz, I. Komaromi, R. Gomperts, R. L. Martin, D. J. Fox, T. Keith, M. A. Al-Laham, C. Y. Peng, A. Nanayakkara, M. Challacombe, P. M. W. Gill, B. Johnson, W. Chen, M. W. Wong, J. L. Andres, C. Gonzalez, M. Head-Gordon, E. S. Replogle and J. A. Pople, *Gaussian 98*, Revision A.11.4, Gaussian, Inc., Pittsburgh PA, 2002.
23 G. Schaftenaar, *Molden v3.6 program*, CMBI, Faculty of Science, University of Nijmegen, The Netherlands, 1999.
24 S. Satyanarayana, J. C. Dabrowiak and J. B. Chaires, *Biochemistry*, 1992, **31**, 9319.
25 S. Satyanarayana, J. C. Dabrowiak and J. B. Chaires, *Biochemistry*, 1993, **32**, 2573.
26 J. G. Liu, Q. L. Zhang, L. N. Ji, Y. Y. Cao and X. F. Shi, *Transition Met. Chem.*, 2001, **26**, 733.
27 X. H. Zou, B. H. Ye, H. Li, Q. L. Zhang, H. Cao, J. G. Liu, L. N. Ji and X. Y. Li, *J. Biol. Inorg. Chem.*, 2001, **6**, 143.
28 J. D. McGhee and P. H. Von Hippel, *J. Mol. Biol.*, 1974, **86**, 469.
29 R. J. Morgan, S. Chatterjee, A. D. Baker and T. C. Strekas, *Inorg. Chem.*, 1991, **30**, 2687.
30 J. G. Liu, Q. L. Zhang, X. F. Shi and L. N. Ji, *Inorg. Chem.*, 2001, **40**, 5045.
31 B. C. Baguley and M. Lebret, *Biochemistry*, 1984, **23**, 937.
32 X. H. Zou, B. H. Ye, H. Li, J. G. Liu, Y. Xiong and L. N. Ji, *J. Chem. Soc., Dalton Trans.*, 1999, 1423.
33 J. G. Liu, B. H. Ye, Q. L. Zhang, X. H. Zou, Q. X. Zhen, X. Tian and L. N. Ji, *J. Biol. Inorg. Chem.*, 2000, **5**, 119.
34 K. Fukui, T. Yonezawa and H. Shingu, *J. Chem. Phys.*, 1952, **20**, 722; G. Klopman, *J. Am. Chem. Soc.*, 1968, **90**, 223; I. Fleming, *Frontier Orbitals and Organic Chemical Reaction*s, Wiley, New York, 1976.